

# Study of $\chi_b$ production at $\sqrt{s} = 7$ and 8 TeV

I. Belyaev<sup>1,2</sup>, C. Bozzi<sup>3</sup>, H. Dijkstra<sup>1</sup>, A. Mazurov<sup>1,4</sup>.

<sup>1</sup>*CERN*, <sup>2</sup>*ITEP, Moscow*, <sup>3</sup>*INFN Sezione di Ferrara*, <sup>4</sup>*Università di Ferrara*

## Abstract

A study of  $\chi_b$  production at LHCb is performed on data collected during 2011 and 2012, by reconstructing  $\chi_b(1P, 2P, 3P) \rightarrow \Upsilon(1S)\gamma$  decays. The differential production cross sections, relative to the  $\Upsilon(1S)$ , are measured as a function of  $\Upsilon(1S)$  transverse momentum and rapidity. The  $\chi_b \rightarrow \Upsilon(2S)\gamma$  and  $\chi_b \rightarrow \Upsilon(3S)\gamma$  decays are also investigated. The  $\chi_b(3P)$  mass is measured.



# 1 Introduction

It is expected that a significant fraction of the production cross-section of  $J/\psi$  and  $\Upsilon$  states in hadron collisions is due to feed-down from heavier quarkonium states. A study of this effect is important for the interpretation of onia production cross section and polarization measurements in hadron collisions. For P-wave quarkonia, measurements of  $\chi_c$  have been reported by CDF [?], HERA-B [?] and LHCb [?], whereas CDF [?] and ATLAS [?] have performed measurements involving  $\chi_b$  states. LHCb has reported [?] a preliminary measurement of the  $\chi_b$  production cross-section, and subsequent decay into  $\Upsilon(1S) \gamma$ , relative to the  $\Upsilon(1S)$  production. This measurement was performed on 2011 data, in a region defined by  $6 \text{ GeV}/c < p_T(\Upsilon(1S)) < 15 \text{ GeV}/c$  and  $2.0 < y < 4.5$ .

This note presents an update of the previous LHCb study. Data collected in 2012 were also analyzed, allowing for cross-section measurements at  $\sqrt{s} = 8 \text{ TeV}$ . Using the full integrated luminosity allows for a measurement of the differential cross-section in  $p_T$  and rapidity bins of the  $\Upsilon(1S)$ , and to study the production of  $\chi_b(2P)$  And  $\chi_b(3P)$ . A measurement of the  $\chi_b(3P)$  mass is also performed by combining data collected in 2011 and 2012.

The analysis proceeds through the reconstruction of  $\Upsilon(nS)$  candidates via their dimuon decays, and their subsequent pairing with a photon to look for  $\chi_b(mP) \rightarrow \Upsilon(nS)\gamma$  decays. Ratios of  $\chi_b(mP)$  to  $\Upsilon(nS)$  production cross section can be written as

$$\frac{\sigma(pp \rightarrow \chi_b(mP) \rightarrow \Upsilon(nS)\gamma)}{\sigma(pp \rightarrow \Upsilon(nS))} = \frac{N_{\chi_b(mP) \rightarrow \Upsilon(nS)\gamma}}{N_{\Upsilon(nS)}} \times \frac{\epsilon_{\Upsilon(nS)}}{\epsilon_{\chi_b(mP) \rightarrow \Upsilon(nS)\gamma}} = \frac{N_{\chi_b(mP) \rightarrow \Upsilon(nS)\gamma}}{N_{\Upsilon(nS)}} \times \frac{1}{\epsilon_{\gamma}^{eco}} \quad (1)$$

where  $N_{\Upsilon(nS)}$  and  $N_{\chi_b(mP) \rightarrow \Upsilon(nS)\gamma}$  are the  $\Upsilon(nS)$  and  $\chi_b(mP)$  yields,  $\epsilon_{\Upsilon(nS)}$  and  $\epsilon_{\chi_b(mP) \rightarrow \Upsilon(nS)\gamma}$  are their corresponding selection efficiencies. The latter are the product of geometric acceptance, trigger efficiency and reconstruction efficiency. Since the selection criteria for the two samples differ only in the reconstruction of a photon, the efficiency ratio can be replaced by  $1/\epsilon_{\gamma}$ , the reconstruction efficiency for the photon from the  $\chi_b$  decay. Similar expressions may be used to compute differential cross sections in  $\Upsilon$   $p_T$  and rapidity bins.

## 2 Data and Monte-Carlo samples

The data sample used in this analysis has been collected by LHCb in 2011 and 2012, at center-of-mass energies of  $\sqrt{s} = 7 \text{ TeV}$  and  $8 \text{ TeV}$ , respectively. For 2011, both Reco12 (?) and Reco14/Stripping 20 samples were used. The former was privately stripped by Vanya (?).

The corresponding integrated luminosities are...

Events are triggered by...

and subsequently stripped by StrippingMicroDSTDiMuonDiMuonIncLine. This line takes StdLooseDiMuon as input, applies requirements on muon momentum, transverse

36 momentum, track and vertex chisquares, and transverse momentum of the composite  
37 particle  
38 `(MINTREE('mu+'==ABSID,PT) > 650.0 *MeV) & (MINTREE('mu+'==ABSID,P)`  
39 `> -8000.0 *MeV) & (MAXTREE('mu+'==ABSID,TRCHI2DOF) < 5.0) & (in_range(`  
40 `3000.0 *MeV, MM, 100000000.0 *MeV)) & (VFASPF(VCHI2PDOF)< 20.0) & (PT >`  
41 `2000.0)`  
42 and saves the output in MicroDST format. The StdLooseDiMuon list contains pairs of  
43 oppositely charged muon from the StdAllLooseMuons list with the additional requirement  
44 CombinationCut (ADOCACHI2CUT(30, ")), MotherCut (VFASPF(VCHI2) ; 25)  
45 Simulated data were produced with 2011 conditions. Six samples of XX million events  
46 each were generated, each corresponding to a different decay under study. Table ??  
47 summarizes the various samples used in this analysis.

### 48 **3 Event Selection criteria**

49 Pairs of opposite charge tracks are used to form  $\Upsilon$  candidates. Both tracks are identified  
50 as muons and must originate from a common vertex Put selection criteria here, discuss  
51 discriminating variables, put all cuts in a table.

### 52 **4 Data - Monte Carlo comparison**

53 A comparison of the distribution of the relevant observables used in this analysis was  
54 performed on real and simulated data, in order to assess the reliability of Monte Carlo in  
55 computing efficiencies. It should be stressed that, since a relative branching fraction is  
56 measured, systematic effects cancel at first order.

57 Combinatorial background has been subtracted in real data by using an *sPlot* technique,  
58 where the discriminant distribution is... The resulting signal weights are used to obtain  
59 the signal distribution for each relevant variable. These distributions are then compared  
60 with simulation, as shown in Figures ??-??. The agreement is generally very good, giving  
61 confidence that the Monte Carlo describes correctly the decays under study.

### 62 **5 Determination of $\Upsilon$ yields**

63 The yields of  $\Upsilon(1S)$ ,  $\Upsilon(2S)$  and  $\Upsilon(3S)$  particles are determined by fitting the dimuon  
64 invariant mass distribution. The combinatorial background is described by... The  $\Upsilon$  peaks  
65 are parameterized with... The  $\alpha$  and  $n$  parameters of the Crystal Ball function are fixed  
66 to... etc... the floating parameters in the fit are... Figure XX and YY show the invariant  
67 mass distribution in 2011 and 2012 data, respectively. The event yields and other fit  
68 parameters are reported in Table ZZ. The systematic uncertainties in the  $\Upsilon$  yields are  
69 determined by... They are discussed in ??.

## 6 Determination of the $\chi_b$ yields

The yields of  $\chi_b(1S, 2S, 3S) \rightarrow \Upsilon(1S) \gamma$  are determined with fits to the  $m(\mu^+\mu^-\gamma) - m(\mu^+\mu^-)$  invariant mass difference. Combinatorial background is described by ..., signal are parametrized with ... Mention how you fix and float the various parameters of this fit... Figure XX and Table YY show the results...

## 7 Determination of selection efficiencies

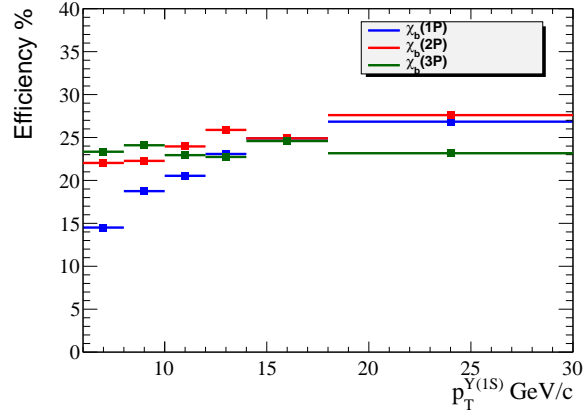


Figure 1: Monte-Carlo data. Fraction of  $\Upsilon(1S)$  originating from  $\chi_b$  decays for different  $p_T^{\Upsilon(1S)}$  intervals.

## 8 Determination of the $\chi_b$ production cross section

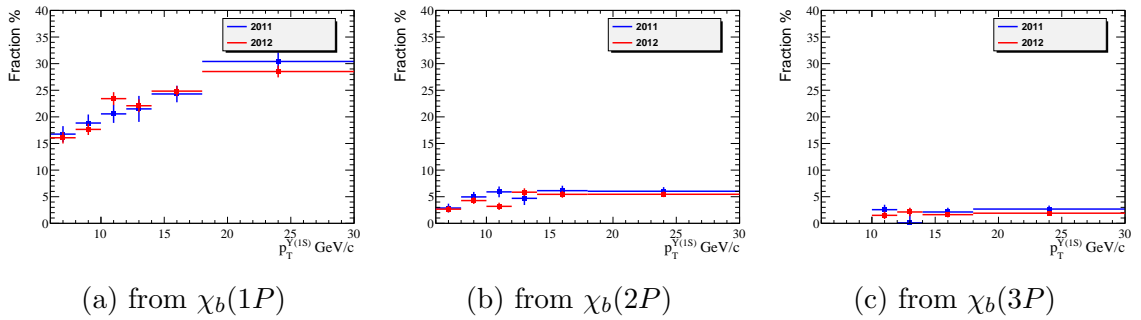


Figure 2: Fraction of  $\Upsilon(1S)$  originating from  $\chi_b$  decays for different  $p_T^{\Upsilon(1S)}$  intervals.

<sup>77</sup> **9**    **Systematic Uncertainties**

<sup>78</sup> **10**   **Determination of the  $\chi_b$  masses**

<sup>79</sup> **11**   **Conclusion**

## 80 Appendices

### 81 A Fitting parameters summary

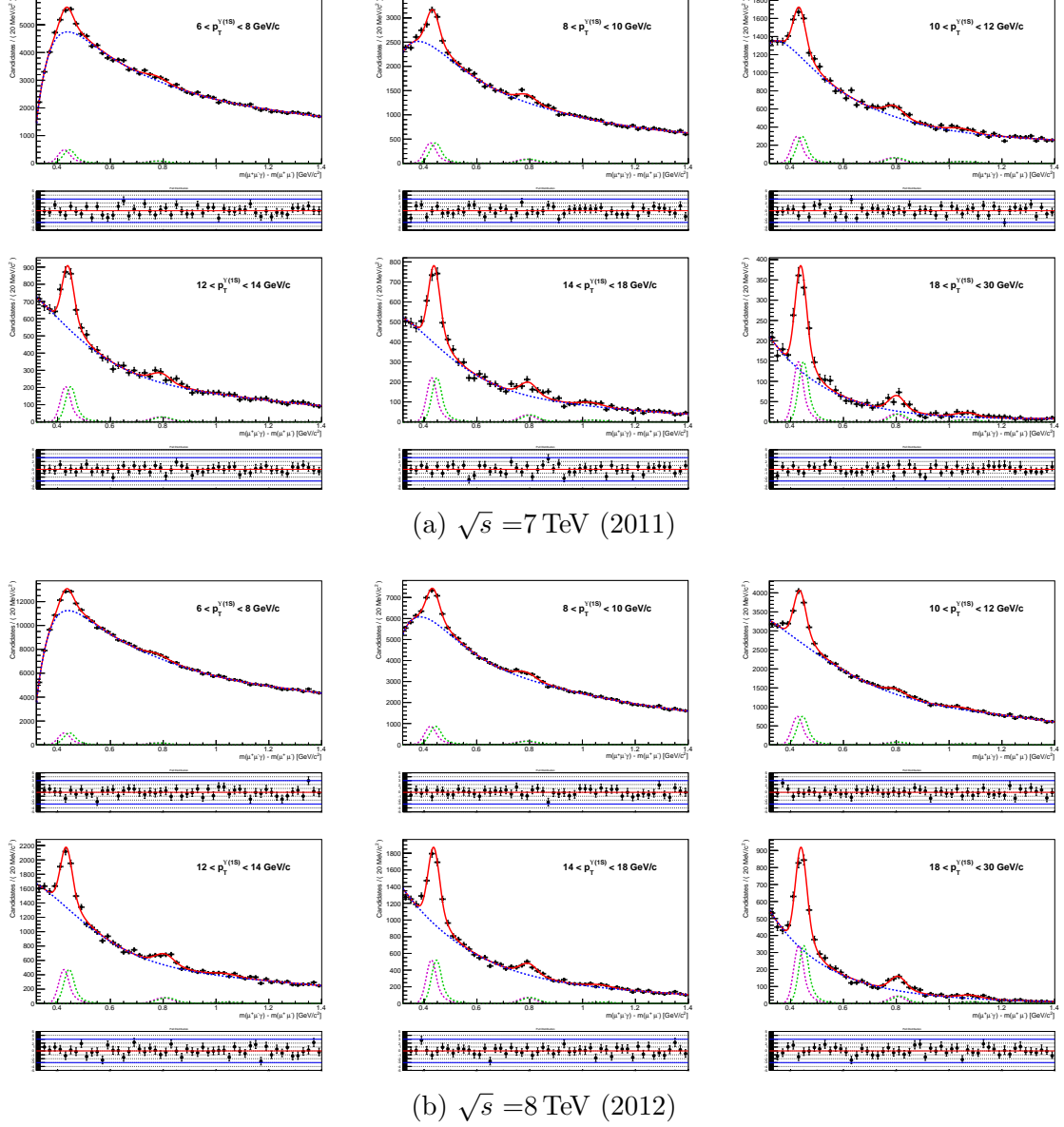


Figure 3: Mass difference of the  $\mu^+\mu^-\gamma$  system and  $\mu^+\mu^-$  system for the data for specified interval of transverse momentum of the  $\Upsilon(1S)$ . The red solid line is the result of the fit described in the text. Blue dashed line is the background contribution obtained from the fit. Magenta and green dashed lines are  $\chi_{b1}$  and  $\chi_{b2}$  signal contribution obtained from the fit.

Table 1: Summary of fraction determination.

	$\bar{T}(1S)$ transverse momentum interval in GeV/c					
	6 - 8	8 - 10	10 - 12	12 - 14	14 - 18	18 - 30
Parameters obtained by fitting data distributions $\sqrt{s} = 7$ TeV						
$N_{\chi_b(1P)}^{rec}$	3130 $\pm$ 280	2610 $\pm$ 220	1750 $\pm$ 140	1130 $\pm$ 130	1190 $\pm$ 80	780 $\pm$ 40
$N_{\chi_b(2P)}^{rec}$	820 $\pm$ 230	820 $\pm$ 150	590 $\pm$ 100	280 $\pm$ 70	300 $\pm$ 50	160 $\pm$ 21
$N_{\chi_b(3P)}^{rec}$			240 $\pm$ 90	0 $\pm$ 140	100 $\pm$ 40	60 $\pm$ 15
$\Delta m_{\chi_{b1}(1P)}$ in MeV/c <sup>2</sup>	425.3 $\pm$ 2.1	424.1 $\pm$ 1.9	424.0 $\pm$ 1.9	430.4 $\pm$ 1.9	429.0 $\pm$ 1.5	429.3 $\pm$ 1.5
$\Delta m_{\chi_{b1}(2P)}$ in MeV/c <sup>2</sup>	770 $\pm$ 12	784 $\pm$ 6	787 $\pm$ 6	786 $\pm$ 13	790 $\pm$ 6	796 $\pm$ 5
$\Delta m_{\chi_{b1}(3P)}$ in MeV/c <sup>2</sup>			1040 $\pm$ 15	1030 $\pm$ 40	1030 $\pm$ 40	1059 $\pm$ 12
$N_{\bar{T}(1S)}^{rec}$	128,900 $\pm$ 400	73,940 $\pm$ 320	41,390 $\pm$ 230	22,790 $\pm$ 170	19,660 $\pm$ 160	9610 $\pm$ 110
Parameters obtained by fitting data distributions $\sqrt{s} = 8$ TeV						
$N_{\chi_b(1P)}^{rec}$	6500 $\pm$ 400	5380 $\pm$ 320	4410 $\pm$ 230	2610 $\pm$ 140	2800 $\pm$ 110	1800 $\pm$ 70
$N_{\chi_b(2P)}^{rec}$	1600 $\pm$ 400	1550 $\pm$ 230	700 $\pm$ 150	780 $\pm$ 100	610 $\pm$ 70	355 $\pm$ 35
$N_{\chi_b(3P)}^{rec}$			320 $\pm$ 150	250 $\pm$ 90	180 $\pm$ 60	104 $\pm$ 22
$\Delta m_{\chi_{b1}(1P)}$ in MeV/c <sup>2</sup>	426.0 $\pm$ 1.6	425.4 $\pm$ 1.4	425.9 $\pm$ 1.1	424.3 $\pm$ 1.2	427.6 $\pm$ 1.0	430.6 $\pm$ 1.0
$\Delta m_{\chi_{b1}(2P)}$ in MeV/c <sup>2</sup>	775 $\pm$ 9	782 $\pm$ 6	795 $\pm$ 9	801 $\pm$ 5	790 $\pm$ 4	801 $\pm$ 4
$\Delta m_{\chi_{b1}(3P)}$ in MeV/c <sup>2</sup>			1043 $\pm$ 19	1031 $\pm$ 27	1061 $\pm$ 16	1074 $\pm$ 4
$N_{\bar{T}(1S)}^{rec}$	277,000 $\pm$ 600	162,500 $\pm$ 500	91,610 $\pm$ 350	51,270 $\pm$ 260	45,350 $\pm$ 240	23,540 $\pm$ 180
Parameters obtained by counting MC matched events for $\chi_{b1}(1P)$ decay						
$N_{\chi_b(1P)}^{MC}$	6172	5345	3653	2266	2131	1113
$N_{\bar{T}(1S)}^{MC}$	42,587	28,398	17,078	9632	8237	3922
$\epsilon_{\chi_{b1}(1P)}^{MC}$ %	14.5	18.8	21.4	23.5	25.9	28.4
Parameters obtained by counting MC matched events for $\chi_{b1}(1P)$ decay						
$N_{\chi_b(1P)}^{MC}$	4327	2676	1298	645	467	164
$N_{\bar{T}(1S)}^{MC}$	29,792	14,325	6594	2850	1952	648
$\epsilon_{\chi_{b1}(1P)}^{MC}$ %	14.5	18.7	19.7	22.6	23.9	25.3
Parameters obtained by counting MC matched events for $\chi_{b1}(2P)$ decay						
$N_{\chi_b(2P)}^{MC}$	4648	3273	2041	1155	1016	524
$N_{\bar{T}(1S)}^{MC}$	20,091	13,810	8176	4426	3974	1898
$\epsilon_{\chi_{b1}(2P)}^{MC}$ %	23.1	23.7	25.0	26.1	25.6	27.6
Parameters obtained by counting MC matched events for $\chi_{b1}(2P)$ decay						
$N_{\chi_b(2P)}^{MC}$	3712	1712	848	431	269	106
$N_{\bar{T}(1S)}^{MC}$	17,731	8212	3694	1679	1110	384
$\epsilon_{\chi_{b1}(2P)}^{MC}$ %	20.9	20.8	23.0	25.7	24.2	27.6
Parameters obtained by counting MC matched events for $\chi_{b1}(3P)$ decay						
$N_{\chi_b(3P)}^{MC}$	4629	3120	1772	1066	884	415
$N_{\bar{T}(1S)}^{MC}$	18,486	12,359	7298	4174	3581	1646
$\epsilon_{\chi_{b1}(3P)}^{MC}$ %	25.0	25.2	24.3	25.5	24.7	25.2
Parameters obtained by counting MC matched events for $\chi_{b2}(3P)$ decay						
$N_{\chi_b(3P)}^{MC}$	2598	1282	524	223	192	49
$N_{\bar{T}(1S)}^{MC}$	12,003	5587	2425	1119	784	232
$\epsilon_{\chi_{b2}(3P)}^{MC}$ %	21.6	22.9	21.6	19.9	24.5	21.1
Average MC efficiency of $\chi_{b1}$ and $\chi_{b2}$ MeV/c <sup>2</sup> in %						
$\epsilon_{\chi_{b1}(1P)}^{MC}$	14.5	18.8	20.5	23.1	24.9	26.8
$\epsilon_{\chi_{b1}(2P)}^{MC}$	22.0	22.3	24.0	25.9	24.9	27.6
$\epsilon_{\chi_{b1}(3P)}^{MC}$	23.3	24.1	22.9	22.7	24.6	23.2
Parameters obtained by fitting MC distributions in MeV/c <sup>2</sup>						
$\Delta m_{\chi_{b1}(1P)}$	428.18 $\pm$ 0.34	427.5 $\pm$ 0.4	427.3 $\pm$ 0.4	427.2 $\pm$ 0.5	427.4 $\pm$ 0.5	428.0 $\pm$ 0.6
$\Delta m_{\chi_{b2}(1P)}$	448.2 $\pm$ 0.5	447.2 $\pm$ 0.6	447.3 $\pm$ 0.7	447.0 $\pm$ 0.9	446.1 $\pm$ 1.1	446.1 $\pm$ 1.4
$\Delta m_{\chi_{b1}(2P)}$	786.4 $\pm$ 0.6	786.5 $\pm$ 0.7	786.7 $\pm$ 0.9	786.5 $\pm$ 1.0	789.0 $\pm$ 1.0	790.2 $\pm$ 1.3
$\Delta m_{\chi_{b2}(2P)}$	800.8 $\pm$ 0.7	800.9 $\pm$ 1.0	799.5 $\pm$ 1.2	802.5 $\pm$ 1.7	799.9 $\pm$ 1.9	802.8 $\pm$ 3.2
$\Delta m_{\chi_{b1}(3P)}$	1046.2 $\pm$ 0.7	1046.8 $\pm$ 0.8	1047.9 $\pm$ 1.0	1047.4 $\pm$ 1.3	1049.5 $\pm$ 1.3	1050.9 $\pm$ 1.9
$\Delta m_{\chi_{b2}(3P)}$	1058.0 $\pm$ 1.0	1055.9 $\pm$ 1.2	1058.1 $\pm$ 2.1	1059.6 $\pm$ 2.8	1063.9 $\pm$ 2.8	1061 $\pm$ 7
$\sigma_{\chi_{b1}(1P)}$	23.14 $\pm$ 0.35	22.3 $\pm$ 0.4	21.1 $\pm$ 0.4	19.9 $\pm$ 0.5	19.4 $\pm$ 0.5	19.0 $\pm$ 0.6
$\sigma_{\chi_{b2}(1P)}$	24.2 $\pm$ 0.5	23.3 $\pm$ 0.6	21.4 $\pm$ 0.7	20.7 $\pm$ 1.0	22.4 $\pm$ 0.9	15.8 $\pm$ 1.3
$\sigma_{\chi_{b1}(2P)}$	34.2 $\pm$ 0.8	33.5 $\pm$ 0.8	32.9 $\pm$ 1.0	32.3 $\pm$ 0.8	30.7 $\pm$ 0.8	29.2 $\pm$ 1.2
$\sigma_{\chi_{b2}(2P)}$	37.5 $\pm$ 0.7	33.5 $\pm$ 1.1	32.6 $\pm$ 1.0	33.1 $\pm$ 1.5	31.6 $\pm$ 1.5	32.1 $\pm$ 2.6
$\sigma_{\chi_{b1}(3P)}$	47.2 $\pm$ 0.6	45.9 $\pm$ 0.7	43.4 $\pm$ 0.9	43.3 $\pm$ 1.1	42.3 $\pm$ 1.0	40.2 $\pm$ 1.5
$\sigma_{\chi_{b2}(3P)}$	49.0 $\pm$ 0.9	42.0 $\pm$ 1.2	43.1 $\pm$ 2.1	40.2 $\pm$ 3.0	38.1 $\pm$ 2.4	41 $\pm$ 6
Fraction of $\bar{T}(1S)$ in % for $\sqrt{s} = 7$ TeV						
from $\chi_b(1P)$	16.8 $\pm$ 1.5	18.8 $\pm$ 1.6	20.6 $\pm$ 1.7	21.5 $\pm$ 2.4	24.3 $\pm$ 1.6	30.4 $\pm$ 1.7
from $\chi_b(2P)$	2.9 $\pm$ 0.8	5.0 $\pm$ 0.9	5.9 $\pm$ 1.0	4.7 $\pm$ 1.3	6.1 $\pm$ 0.9	6.0 $\pm$ 0.8
from $\chi_b(3P)$			2.6 $\pm$ 0.9	0.1 $\pm$ 2.7	2.1 $\pm$ 0.8	2.7 $\pm$ 0.7
Fraction of $\bar{T}(1S)$ in % for $\sqrt{s} = 8$ TeV						
from $\chi_b(1P)$	16.1 $\pm$ 1.1	17.6 $\pm$ 1.1	23.4 $\pm$ 1.2	22.1 $\pm$ 1.2	24.8 $\pm$ 0.9	28.5 $\pm$ 1.1
from $\chi_b(2P)$	2.7 $\pm$ 0.6	4.3 $\pm$ 0.6	3.2 $\pm$ 0.7	5.9 $\pm$ 0.7	5.4 $\pm$ 0.6	5.5 $\pm$ 0.5
from $\chi_b(3P)$			1.5 $\pm$ 0.7	2.1 $\pm$ 0.8	1.6 $\pm$ 0.5	1.9 $\pm$ 0.4



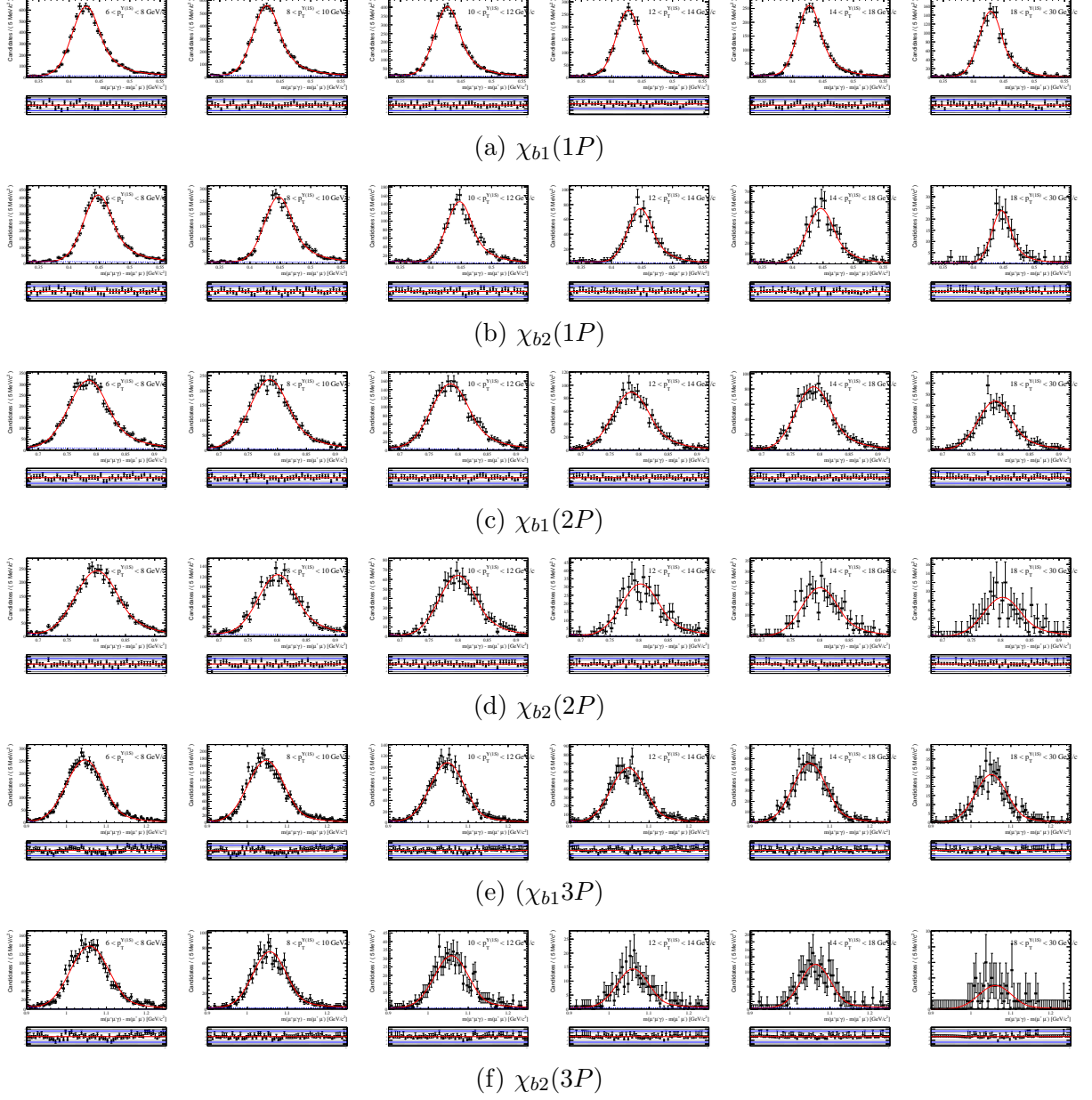


Figure 4: Mass difference of the  $\mu^+\mu^-\gamma$  system and  $\mu^+\mu^-$  system for the Monte Carlo data for specified interval of transverse momentum of the  $\Upsilon(1S)$ . The red solid line is the result of the fit described in the text.